Automated Volumetric Surveillance of Primary and Postoperative Type B Aortic Dissection

Alice Maccarini[1], Marco Ferraresi[2], Alessandro Molinari[2], Janko Jovanovic[2], Luca Mainardi[3], Pietro Cerveri[1]

[1] Università di Pavia, Pavia, Italy
[2] ASST Lecco, Lecco, Italy
[3] Politecnico di Milano, Milan, Italy

Abstract

Automated volumetric surveillance of Type B aortic dissection (TBAD) is limited by manual segmentation overhead (60–75 min) in computed tomographic angiography (CTA). We propose AORTA-SCAN, a hierarchical deep-learning network designed to identify the true and false lumina of the aortic dissection (AD) in both primary and post-TEVAR CTA. In addition to the traditional 1D biomarker, aortic diameter, the framework provides the Perfusion Dissection Index (PDI), a 3D clinical indicator of aortic remodeling. The proposed model shows a significant improvement in FL Dice (0.84 vs 0.71, $p < 0.001$) compared with a 3D U-Net baseline and high agreement for the PDI, with a mean bias of (-0.17%) relative to the expert reference. The pipeline reduces processing time to about 10 minutes, supporting scalable 3D volumetric surveillance.

1. Introduction

Type B aortic dissection (TBAD) is a critical pathology characterized by an intimal tear creating a false lumen (FL) alongside the true lumen (TL). While current clinical guidelines rely on maximum aortic diameter to guide intervention, this 1D metric fails to capture the 3D complexity of the disease [1]. Consequently, volumetric indices such as the Perfusion Dissection Index (PDI) [2] and regional TL collapse metrics [3] have gained interest as indicators of aortic remodelling. However, their clinical integration is obstructed by the high manual overhead of 3D segmentation in computed tomographic angiography (CTA), taking on average about 60–75 min, and the failure of standard automated pipelines in the presence of metallic beam-hardening artifacts from thoracic endovascular aortic repair (TEVAR) [4]. Despite advances in deep learning for aortic segmentation [5], a significant translational gap remains due to the scarcity of publicly available TBAD data and the absence of postoperative datasets for model validation. To address these challenges, we propose AORTA-SCAN, an automated hierarchical deep learning network for volumetric surveillance of both primary and postoperative CTA. The approach employed a hierarchical strategy that decouples global localization from fine-grained lumen analysis to maximize computational efficiency. We implemented a domain adaptation strategy based on sequential transfer learning and partial-label supervision to address differences in image characteristics and annotation coverage across public and clinical datasets.

2. Materials and Methods

2.1. Data Strategy and Processing

Five datasets with complementary characteristics were integrated into a multi-stage training pipeline (Table 1, Fig. 1). Coarse localization (SEG1) used AortaSeg24 [6] (D1) to isolate the global vessel volume, reducing the search space for subsequent stages. Initial TL/FL training (SEG2) leveraged 100 TBAD CTAs from ImageTBAD [7] (D2), where false lumen thrombus (FLT) labels were consolidated into the FL class for consistency. To extend coverage across thoracic and abdominal aortic segments, SEG3 incorporated the Graz University dataset (D3) [8]. Final domain adaptation (SEG4a and SEG4b) targeted clinical preoperative and postoperative CTA scans from ASST Lecco (D4a, D4b). For postoperative scans (D4b), where metallic stent labels were unavailable, high-attenuation thresholding (> 800 HU) provided a physical surrogate to train a triple-input architecture, enabling the model to differentiate intra-stent space from extra-stent lumina despite beam-hardening artifacts. CTA volumes were standardized using the MONAI framework [9], including isotropic resampling ($1.0\ mm^3$) and RAS reorientation. For coarse localization, intensities were clipped to a vascular range (-200 to $+600$ HU). Fine-grained segmentation exploits

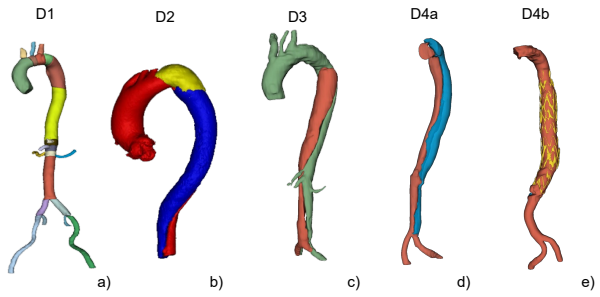

Figure 1. **3D AD datasets.** D1: AortaSeg24, 24 anatomical classes, [6]; D2: ImageTBAD, FL, TL, and FLT [7]; D3: Graz University cohort, TL and FL, [8]; D4a: preoperative ASST Lecco; D4b: postoperative ASST Lecco.

a multi-windowing approach: preoperative scans used a dual-channel input consisting of a vascular channel (-200 to $+1500$ HU, 0.5%–99.5% percentile scaling, adaptive histogram equalization) and a probabilistic Gaussian soft-prior. For postoperative scans, a third metal-sensitive channel ($+600$ to $+2000$ HU) was added to localize stent grafts and mitigate beam-hardening artifacts. All channels were normalized using instance-wise Z-scores. Training employed a patch-based strategy (128^3 voxels) with class-specific weighting to address imbalance. On-the-fly 3D data augmentation included spatial transformations (flipping, 90° rotations, $p = 0.4$) and intensity adjustments (gamma contrast $\gamma \in [0.5, 1.5]$, Gaussian noise $\sigma = 0.1$, and smoothing $\sigma \in [0.5, 1.0]$). Intensity augmentations were restricted to image channels to preserve the structural integrity of the soft-prior input.

2.2. Hierarchical Framework and Stent-Aware Modeling

The framework decouples global localization from fine-grained analysis. A coarse module identifies the aortic ROI and generates a probabilistic soft-prior to guide the second-stage segmentation of the TL and FL. For post-TEVAR surveillance, a triple-input architecture explicitly models the stent as a separate class. By isolating metallic components, the framework restricts V_{TL} to the intra-stent compartment, neutralizing blooming artifacts that typically obscure the intimal flap. Domain adaptation was performed through sequential transfer learning from the comprehensively annotated public datasets to the partially annotated ASST Lecco cohorts. Since the clinical annotations included only the anatomical regions relevant to the local surveillance protocol, a spatial supervision mask was used to distinguish annotated regions from regions without reliable reference labels. The partial-label loss therefore quantified segmentation performance only within the annotated area, preventing structures omitted from the clinical masks from being automatically treated as background.

Table 1. Framework Development Stages and Dataset Roles.

Stage	Dataset	N	Target Class	Focus
SEG1	D1	50	Aorta	Coarse Localization
SEG2	D2	100	TL, FL, B	Initial Segmentation
SEG3	D3	40	TL, FL, B	Anatomical Extension
SEG4a	D4a	10	TL, FL, B	Primary Refinement
SEG4b	D4b	19	TL, FL, B, S	Stented Robustness

2.3. Geometric Analysis and Evaluation

PDI clinical biomarker was quantified as $PDI = V_{FL}/(V_{TL} + V_{FL})$ [2]. It was computed via graph-based topological analysis of the TL and FL reconstructed surfaces. A 3D centerline was generated via skeletonization to calculate the equivalent diameter $D_{eq} = 2\sqrt{A/\pi}$. Performance was validated via 5-fold cross-validation using Dice coefficients, relative volumetric error (RVE), linear regression, and Bland-Altman analysis.

2.4. Implementation Details

The framework was implemented in PyTorch using MONAI. Fine-grained segmentation uses the CAREUNet (a 3D U-Net [10] variant) to integrate probabilistic soft priors and resolve intimal-flap textures. Training was performed on an NVIDIA H100 GPU (80 GB VRAM) using the AdamW optimizer (learning rate 1×10^{-4}, weight decay 1×10^{-5}). We employed a generalized Dice loss for stages SEG1–SEG3. For domain adaptation on SEG4a–SEG4b, the Dice–cross-entropy loss was evaluated only within the clinician-annotated region, so that anatomy omitted from the partial Lecco annotations did not contribute to the optimization. Models used a patch-based strategy (128^3 voxels), with selection based on the highest validation Macro Dice score. The end-to-end automated pipeline processes a case in under 10 minutes.

The 3D U-Net baseline was trained using the same data and training protocol as CAREUNet, differing only in network architecture.

3. Results

3.1. Segmentation Performance and Benchmark Validation

AORTA-SCAN demonstrated a significant performance gain over the 3D U-Net baseline [10] when validated against the manual expert ground truth (Tab. 2). As the table shows, AORTA-SCAN significantly outperformed the 3D U-Net baseline across all global and class-specific metrics. Notably, FL Dice significantly improved from 0.71 to 0.84 ($p < 0.001$), while specificity remained > 0.99,

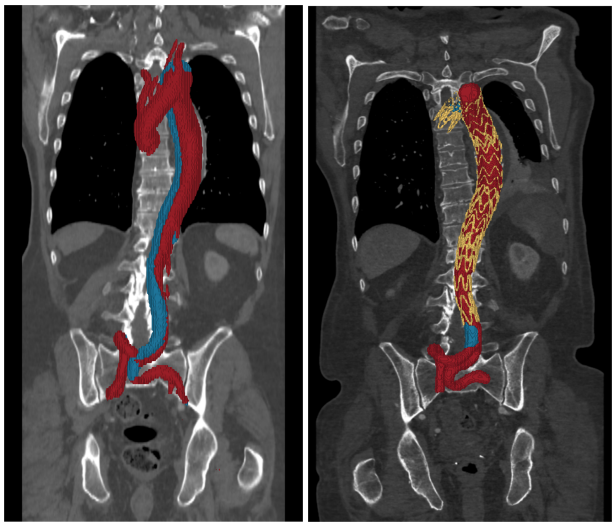

(a) preoperative segmentation (b) postoperative segmentation

Figure 2. **3D Aortic Reconstructions.** (a) preoperative dissection; (b) postoperative remodeling.

ensuring conservative boundary definition to prevent diameter overestimation. The model generalized effectively to the ASST Lecco clinical dataset (Fig. 2a), achieving masked Dice scores of 0.78 (TL) and 0.72 (FL). Qualitative assessment confirmed that the Gaussian soft-prior supported intimal flap delineation even in cases of severe luminal compression. In the stented cohort ($N = 19$), the triple-input architecture successfully isolated metallic components, achieving a Dice score for stent equal to 0.70, maintaining high accuracy for stented lumina with TL Dice of 0.90 and FL Dice of 0.75. However, a trade-off of the clinical domain adaptation was observed in the postoperative scans (Fig. 2b). As the expert ground truth excluded the ascending aorta, the network specialized in the stented descending region while losing the ability to segment the aortic arch. Despite this localized shift, the results confirmed the framework's robustness against beam-hardening artifacts and its fidelity to the clinical surveillance protocols provided by the medical center.

3.2. Clinical Validation and Geometric Analysis

Linear regression (Fig. 3a) showcased agreement between automated predictions and the manual expert ground truth. Results showed concordance with FL volumes ($r = 0.97$), whereas the lower TL correlation ($r = 0.52$) reflected the high specificity required in distal regions. This conservative boundary definition was further evidenced by the preoperative masked RVE, which reached -10.91% for the TL and -13.76% for the FL. For the postoperative cohort, correlation improved significantly (mean $r = 0.96$ for stented lumina). Bland-Altman analysis

Table 2. Comparative performance on the Graz Dataset ($N = 40$). Results represent mean values; p-values are derived from the paired Wilcoxon signed-rank test comparing AORTA-SCAN (B) against the 3D U-Net baseline (A).

Metric	Class	A	B	p-value
Dice Score	**Global**	0.810	0.853	3.20×10^{-6}
	True Lumen	0.754	0.816	3.01×10^{-5}
	False Lumen	0.707	0.837	5.26×10^{-8}
Precision	**Global**	0.765	0.836	8.39×10^{-7}
	True Lumen	0.810	0.855	0.009
	False Lumen	0.722	0.819	2.09×10^{-7}
Sensitivity	**Global**	0.726	0.836	6.77×10^{-7}
	True Lumen	0.732	0.796	0.005
	False Lumen	0.720	0.875	1.94×10^{-7}
Specificity	**Global**	0.998	0.998	2.11×10^{-5}

(Fig. 3b) confirmed minimal systematic bias relative to manual ground truth. Notably, the PDI absolute error of 0.051 significantly improved upon the 3D U-Net baseline error (0.087, $p = 0.025$). The negligible mean PDI difference (-0.17%) and precise automated extraction of the equivalent diameter (D_{eq}) facilitated integrated 1D and 3D geometric monitoring in a single clinical pipeline. For the postoperative scenario, the framework achieved a mean absolute PDI error of 0.010 and a mean RVE of 0.078. These results substantiated that, while voxel-wise segmentation varies across complex cases, the global volumetric indices remained stable across different clinical acquisitions.

4. Discussion

AORTA-SCAN generated a comprehensive volumetric analysis in under 10 minutes, representing an 85% reduction in processing time compared to manual segmentation. A core strength of the framework is the prioritization of precision over sensitivity; by maintaining a specificity > 0.99, the Gaussian prior prevents aortic diameter overestimation. Methodologically, the hierarchical approach optimizes the computational footprint, allowing the CAREUNet to resolve subtle textural differences in the intimal flap. Compared to the 3D U-Net baseline, our framework demonstrated significant sensitivity and Dice improvements ($p < 0.001$), proving more reliable for complex pathology.

While absolute TL volume showed moderate correlation ($r = 0.52$) due to conservative distal under-segmentation, evidenced by the negative RVE bias, the PDI remained remarkably stable. The negligible mean difference (-0.17%) and reduced absolute error confirm the framework's utility as a high-fidelity surrogate for luminal compression. Furthermore, the triple-input architecture successfully neutralized beam-hardening artifacts in postoperative scans; the high stented TL Dice (0.90) and

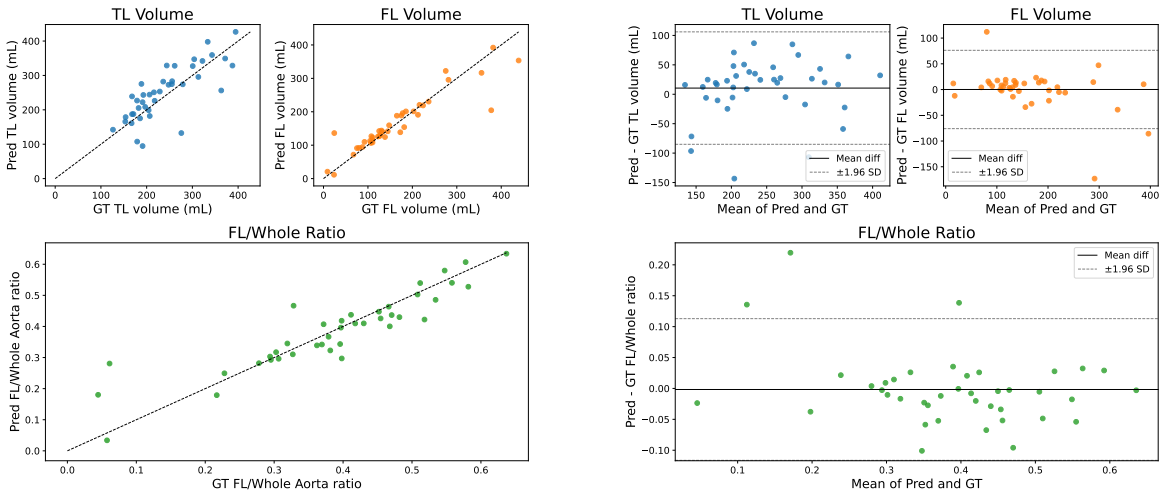

(a) Linear Regression

(b) Bland-Altman

Figure 3. **Volumetric Validation.** (a) Scatter plots demonstrate consistency for FL volumes ($r = 0.97$) and PDI ($r = 0.94$). (b) Bland-Altman analysis confirms minimal systematic bias (PDI mean difference: -0.17%).

correlation ($r = 0.96$) confirm that explicitly modeling the metallic mesh effectively partitions compartments for monitoring remodeling. Furthermore, the low PDI error (0.010) is crucial, since in clinical post-TEVAR it has been shown that a PDI ≥ 0.1 might point to the need for reintervention [2]. On the other hand, for primary TBAD, PDI might become a tool to longitudinally monitor the pathology to early identify malperfusion cases or severe disease progression.

Data scarcity remains a primary constraint, particularly for stented cohorts. Future developments will focus on mitigating clinical labeling bias to restore aortic arch segmentation in postoperative scans. Additionally, we aim to implement automated zonal analysis for regional PDI calculations [2] and a human-in-the-loop platform to integrate AI efficiency with expert clinical oversight.

5. Conclusion

AORTA-SCAN provides a robust solution for automated TBAD surveillance across primary and postoperative domains. By delivering stable volumetric biomarkers like the PDI in a fraction of the time required for manual analysis, this hierarchical approach supports the clinical transition from 1D diameter-based monitoring to comprehensive 3D hemodynamic assessment.

Acknowledgments

This work is partially funded by ASST Lecco Alessandro Manzoni.

References

[1] D'Oria M, et al. Critical review of guidelines for type b aortic dissection. Ann Vasc Surg May 2025;114:380–390.

[2] Ferraresi M, et al. Volumetric analysis in primary and residual type b aortic dissection... can predict aortic reintervention. J Vasc Surg Jun. 2024;79(6):1315–1325.

[3] Li Y, Yuan G, Zhou Y. The value of volume measurement in ct in the follow-up of stanford b aortic dissection after tevar. BMC Cardiovasc Disord Nov. 2024;24(1).

[4] Romeiro AB, et al. Predictors of adverse events in uncomplicated type b aortic dissection: a systematic review with meta-analysis. Int Angiol Oct. 2021;40(5).

[5] Pepe A, et al. Detection, segmentation, simulation and visualization of aortic dissections: A review. Med Image Anal Oct. 2020;65:101773.

[6] Imran M, et al. Multi-class segmentation of the aorta: Aortaseg 2024 challenge. Springer, 2026; .

[7] Yao ZY, et al. Imagetbad: A 3d computed tomography angiography image dataset for automatic segmentation of type-b aortic dissection. Front Physiol Sep. 2021;12.

[8] Mayer C, et al. Aortic dissection dataset and segmentations, 2024.

[9] Cardoso MJ, et al. Monai: An open-source framework for deep learning in healthcare. arXiv:2211.02701, 2022.

[10] Çiçek Ö, et al. 3D U-Net: Learning Dense Volumetric Segmentation from Sparse Annotation. Springer, 2016; 424–432.

Address for correspondence:

Alice Maccarini
Via Adolfo Ferrata 5, 27100, Edificio La Nave, Pavia, Italy
alice.maccarini01@universitadipavia.it